

Moritz Schaar*, Thorsten M. Buzug and Magdalena Rafecas

PET image reconstruction using the Origin Ensemble algorithm and geometric constraints

Abstract: The *Origin Ensemble* method allows image reconstruction of photon-limited emission tomography data to be performed entirely in the image domain. This offers attractive perspectives such as including scatter events for image reconstruction in *Positron Emission Tomography*. In this work, the probability of single Compton scatter along a line-of-response is estimated by the *Single Scatter Simulation* algorithm; for every event a decision is made whether this event is reconstructed along a line or an area confined by two circular arcs holding potential scatter points. First results of 2D simulations show visual agreement with the reference and locally increased *contrast recovery coefficient* values.

Keywords: positron emission tomography, scatter correction, single scatter simulation, origin ensemble, maximum likelihood expectation maximization

<https://doi.org/10.1515/cdbme-2017-0115>

1 Introduction

Positron Emission Tomography (PET) is a powerful functional imaging technique based on the injection of a radioactive tracer into the patient. As a consequence of radioactive decay and subsequent annihilation of the emitted positron, pairs of anti-parallel photons are emitted. The image formation process is driven by the detection of the photons pairs that emerge in the vicinity of the tracer, so that the reconstructed image is an estimate of the tracer distribution. Photoelectric absorption and Compton scatter are the main physical interactions of the photons within the

patient and a significant source of image degradation. Photoelectric absorption results in an intensity loss and reduced signal-to-noise ratio. On the other hand, scatter introduces counts in areas where no activity should be present and it is thus a source of image noise. Currently, there are several methods to correct for scatter. These methods require the estimation of the scatter contribution which is taken into account as a noise contribution in the forward-projection step of statistical iterative reconstruction. On the contrary, the approach at hand considers scatter events as an additional signal source instead of correcting for scatter effects. Thereby a novel statistical method called *Origin Ensemble* (OE) is used. One advantage of OE is that the reconstruction is performed entirely in the image domain, i.e. without time consuming forward and backprojection operations.

In standard OE image reconstruction for PET without time-of-flight information, it is assumed that the emission must have occurred somewhere along the line connecting two detectors in coincidence. Considering single Compton scatter within the subject enlarges the region where the photons could have originated. More precisely, for single scattered events and a 2D object, the area is constrained by two arcs holding potential scatter points. The arcs depend on the energy of the detected event. To the best of the authors' knowledge, this is the first contribution that demonstrates the use of scatter events in OE image reconstruction instead of scatter correction.

This paper shows first results based on simulations in 2D and the differences between standard iterative image reconstruction and OE reconstruction are outlined.

2 Methods

2.1 Origin ensembles

The Origin Ensemble method has been suggested by Sitek in [1] as an alternative formalism of the image reconstruction process of photon-limited tomographic data. Usually,

*Corresponding author: **Moritz Schaar:** Institute of Medical Engineering, University of Lübeck, Ratzeburger Allee 160, 23562 Lübeck, Germany, e-mail: schaar@imt.uni-luebeck.de

Thorsten M. Buzug, Magdalena Rafecas: Institute of Medical Engineering, University of Lübeck, Ratzeburger Allee 160, 23562 Lübeck, Germany, e-mail: buzug@imt.uni-luebeck.de, rafecas@imt.uni-luebeck.de

iterative approaches like the *maximum likelihood expectation maximization* (MLEM) algorithm in combination with accurate models of the measurement process are used to estimate the activity distribution inside the object. The OE method follows a different approach by stochastically estimating the number of emissions per voxel directly in the image domain.

OE for PET data usually operates on lines connecting two detectors in coincidence, the so-called *line-of-response* (LOR). A simplified version of the algorithm for LOR-based reconstruction might be formulated as:

1. *Initialization*: For each event randomly distribute the expected point of photon emission along the LOR. Count all events per image pixel to get an initial density matrix \mathbf{D} .
2. Randomly select one event and chose a new position along the corresponding LOR.
3. The new position will be accepted with probability equal to:

$$\min\left(1, \frac{(d_{new}+1)\epsilon_{old}}{d_{old}\epsilon_{new}}\right). \quad (1)$$

Here, d_{old} , d_{new} are the densities and ϵ_{old} , ϵ_{new} are the sensitivity values at the old respectively new position.

4. If the new position is accepted, the event is moved to this position and the density matrix is updated.
5. Repeat steps 2)-5).

One full OE iteration is completed when all events have been inspected once. Thus, every iteration generates a new state of a Markov chain. After several iterations, this chain reaches equilibrium where the average number of emissions per voxel is independent of the iteration. Averaging the set of states at the end of the chain results in an estimate of the average number of emissions per voxel. The typical number of iterations is in the order of several thousands.

2.2 Compton scatter in positron emission tomography

In PET imaging, the emitted photons may interact with electrons of the tissue and either get absorbed by photoelectric absorption or deviate from the original trajectory by Compton interactions. In the case of Compton scatter, the photon loses part of its energy. In principle, multiple orders of scattering are possible, but with increasing scatter order the probability of detecting the photon decreases.

The common approach for scatter correction is to add an estimation of the scatter contribution to each LOR in the

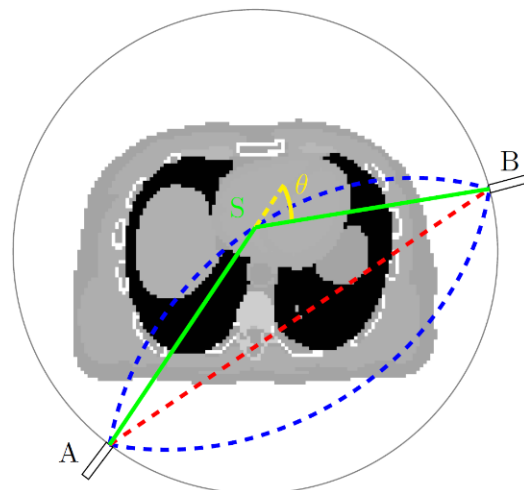


Figure 1: Visualization of one slice of the XCAT attenuation phantom and a PET scanner with two detectors in coincidence. Red dashed line: LOR of both detectors. Blue arcs: limits of the possible scatter locations for a given energy which is directly related to the scatter angle (highlighted in yellow). The emission must have occurred somewhere along the green lines and then scattered at one position of the upper arc inside the body contour.

forward projection step of an iterative image reconstruction like MLEM. This estimation can be calculated by the *Single Scatter Simulation* (SSS) [2]. Due to the inherently different nature of the OE method, SSS cannot be applied directly during image reconstruction. However, SSS can be used as an additional source of information to include scatter in the image reconstruction.

2.3 Scatter modelling in OE

In [3], Sitek and Kadrmas suggested to estimate the contribution of scatter for each LOR using expected values:

$$\pi_i = \frac{E[s_i]}{E[t_i + s_i + r_i]}, \quad (2)$$

where $E[t_i]$, $E[s_i]$ and $E[r_i]$ are the expected values of true, scatter and random events along LOR i , respectively. The contribution of random events will not be further considered here. The scatter estimation is calculated using the SSS approach. Expected values of all contributions as used in the denominator of (2) can either be generated by forward projection of a scatter corrected image generated by MLEM with SSS and applying the scatter estimation, or directly from the measured data.

In OE, a Bernoulli trial with probability π_i is performed every time an event is inspected and depending on the classification of the event as scatter, the event is temporarily

removed from the data during one iteration [3]. After this iteration, the event is automatically re-added to its former location and a new trial is performed when the event is inspected again. Instead of removing scatter events, we propose to use these events by adjusting the area which this event is reconstructed into.

Knowing the energy of detected photons allows the scatter angle θ for a single Compton scatter interaction to be calculated as:

$$\cos(\theta) = 2 - \frac{E_0}{E_s}, \quad (3)$$

where E_0 is the energy of the photon before and E_s the energy after the Compton interaction. For two detectors in coincidence and a fixed energy of the detected photon, potential scatter positions can be found along two circular arcs connecting both detectors as shown in **Figure 1**, [4]. This extends possible emission positions from a line to an area enclosed by both arcs. For each event marked as scatter by the Bernoulli trial, the event is randomly distributed in the intersection area confined by the two circular arcs and the body contour. The body contour is usually known from an additional PET transmission or CT scan. If an event is considered as a true one, we follow the classic distribution along the LOR.

3 Results

3.1 Simulations

A 2D clinical PET scanner was simulated using the *Geant4 Application for Tomographic Emission* (GATE, v7.2) [5]. The simulated system had an inner diameter of 458 mm and 644 *Lutetium Oxyorthosilicate* (LSO) crystals distributed in 28 blocks around the gantry. Simulations of one slice of the *XCAT* torso emission and attenuation phantom [6] were performed. No energy or spatial blurring was applied. In total $3.9 \cdot 10^9$ simulated photon pairs were emitted and the data were filtered to only contain single Compton scattered and true events. Due to the nature of Compton scatter being a process in three dimensions, the in-plane scatter contribution is extremely low. For the sake of demonstration, the spectrum of the data has been modified to have an artificial scatter fraction of 50% by combining the available scatter events with equal amount of randomly selected true events. This is a rather practical consideration and can be seen as a rough approximation of a highly scattering media in 2D. For all reconstruction types, the same set of $4.5 \cdot 10^5$ detected events has been used.

3.2 Image reconstructions

To investigate the effects of the proposed method, three different reconstruction methods are compared. As reference, the standard MLEM reconstruction with attenuation correction and scatter correction based on SSS is used. Additionally, two OE variants have been implemented: (a) with temporary scatter removal and, (b) the proposed method. In contrast to the other two, the later includes the modelling of scatter and subsequent reconstruction using two circular arcs.

The convergence of the OE method has been verified in terms of the systems entropy as suggested by Wülker [7]. The entropy of each state of the Markov chain is calculated as:

$$\mathcal{H} = - \sum_j \frac{d_j}{K} \log \frac{d_j}{K}, \quad (4)$$

where d_j is the number of events at pixel j and K is the total number of events. The entropy over iterations is shown in **Figure 2**. It can be seen that the arc-based approach reaches equilibrium after the LOR method as the number of possible locations in space is significantly increased. Based on **Figure 2**, the last 1000 states of 10000 iterations have been averaged.

For comparison of MLEM with OE, MLEM was terminated when the *signal-to-noise ratio* (SNR), calculated as fraction of mean intensity value and standard deviation in a *region of interest* (ROI) reached the same level as the OE reconstruction with arcs. The ROI used is given by the black outline in **Figure 3 (a)**. All reconstructions were performed on a 90x90 pixel grid with 3.91 mm isotropic pixel length and post-smoothed using a Gaussian filter with standard deviation of 0.5 pixel.

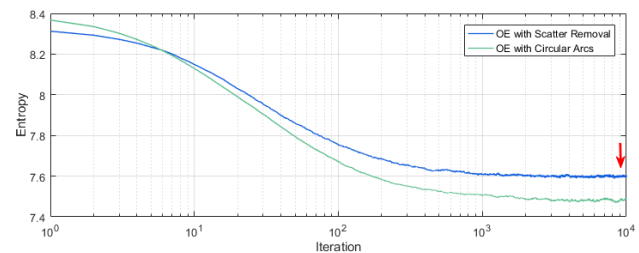


Figure 2: Entropy of both OE methods over iterations. The red arrow indicates the start of the averaging process.

3.3 Simulation results

For all detected counts, the emission position has been calculated and depicted in **Figure 3 (a)**. The reconstruction

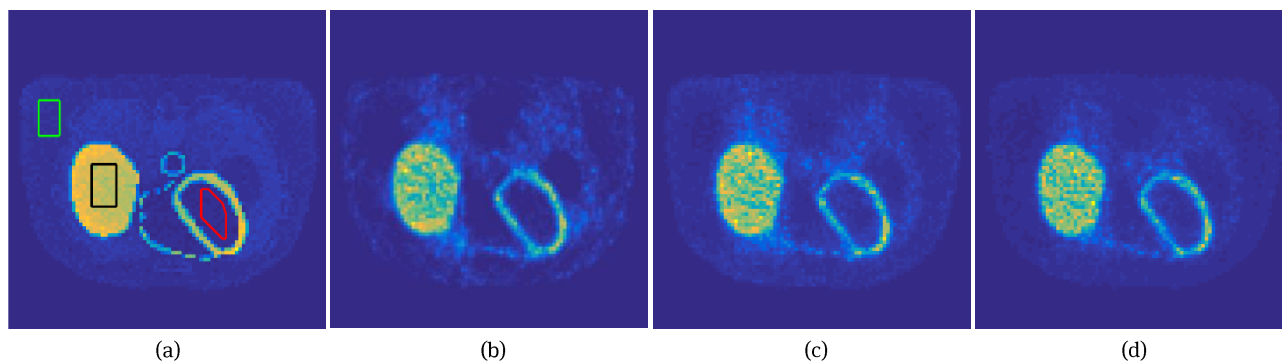


Figure 3: Emission phantom of all events used for reconstruction (a) reconstruction results for MLEM with 55 iterations and SSS-based scatter correction (b), OE with scatter removal (c) and OE with the proposed circular arcs method (d).

results of all three methods are shown in **Figure 3 (b)-(d)**. Whereas both OE methods perform similarly, MLEM suffers from serious fluctuations in the homogeneous area towards the body contour. All three reconstructions lack some details like the aorta or the sharp edges of the heart as typical for the low resolution of PET. Taking a closer look at both OE variants, the area next to the liver becomes unclear when using scatter correction. Furthermore, the outline of the heart in the centre left gets slightly broader than in the reconstruction using arcs.

For quantitative analysis, the *contrast recovery coefficient* (CRC) has been calculated as:

$$\text{CRC} := \frac{(H/C)_{\text{recon}} - 1}{(H/C)_{\text{phantom}} - 1}, \quad (5)$$

where H and C are the mean intensity values in the hot and cold areas of the image, respectively the corresponding area in the reference phantom. CRC is a measure of the contrast of the reconstruction in relation to the targeted contrast given by the emission phantom. **Figure 3 (a)** shows the three ROI's used for CRC calculation: one hot area in black, one cold area inside the heart in red and a second cold area in the soft tissue in green. The results of SNR and CRC for all ROIs are listed in **Table 1**. The reference ratio used in the denominator of (5) corresponds to approximately 37.35.

Whereas the SNR values only differ marginally, the CRC comparison between the red and the black area indicates that MLEM reconstructs both areas very well. On the contrary, both OE methods do not perform sufficiently in this case. The results between the green and the black ROI demonstrate, that MLEM is not able to reconstruct the correct

activity distribution in the soft tissue and thus exceeds the targeted CRC value of one. Here, the OE method using circular arcs performs best in contrast to the other methods.

4 Conclusion

This paper presents an approach to model and utilize scatter in the novel image reconstruction technique OE for photon-limited data. The feature of the OE method to perform image reconstruction entirely in the image domain opens new perspectives in modelling the imaging process. Preliminary results performed on simulations indicate that this approach might be possible to generate more accurate reconstructions with reduced scatter contributions and thus eliminate the need for scatter correction. Future research on this topic will include additional image degrading effects as limited energy resolution of the PET scanner and the extension to 3D. Furthermore, different acceptance ratios in the process of generating states of the Markov chain will be investigated.

Acknowledgment: The authors acknowledge the North-German Supercomputing Alliance (HLRN) for providing HPC resources that have contributed to the research results reported in this paper.

Author's Statement

Research funding: The authors state no funding involved. Conflict of interest: Authors state no conflict of interest. Informed consent: Informed consent is not applicable. Ethical approval: The conducted research is not related to either human or animals use.

Table 1: Comparison of the reconstruction methods in terms of SNR and CRC in different regions of interest according to **Figure 3 (a)**.

Reconstruction	SNR	CRC _{red}	CRC _{green}
MLEM (55 iterations)	3.04	0.81	1.27
OE with scatter removal	3.16	0.39	0.72
OE with arcs	3.04	0.42	0.91

References

- [1] Sitek A, Phys Med Biol 2008;53(12):3201–3216.
- [2] Werling A, et al., Phys Med Biol 2002;47(16):2947–2960.

- [3] Sitek, A and Kadrmas DJ, Proc Ful Three-Dim Imag Reconstruct Radiol Nucl Med Germany, 2011;11:163–1661.
- [4] Conti M et al., Phys Med Biol 2012;57(15):N307–N317.
- [5] Jan S et al., Phys Med Biol 2004;49(19):4543–4561.
- [6] Segars W et al., Med Phys 2010;37(9):4902–4915.
- [7] Wülker C et al., Phys Med Biol 2015;60(5):1919-1944.